I S A V

Journal of Theoretical and Applied Vibration and Acoustics

journal homepage: http://tava.isav.ir

Wave propagation analysis of magneto-electro-thermo-elastic nanobeams using sinusoidal shear deformation beam model and nonlocal strain gradient theory

Ahad Amiri, Arian Masoumi, Roohollah Talebitooti*, Mir Saeed Safizadeh

School of Mechanical Engineering, Iran University of Science and Technology, Narmak, 16765-163, Tehran, Iran

ARTICLE INFO

Article history:
Received 7 March 2019

Received in revised form
5 June 2019

Accepted 23 October 2019

Available online 11 November 2019

Keywords:
Wave propagation,

Nonlocal and length-scale parameters,

Escape frequency,

Cut-off wave number,

Cut-off frequency.

ABSTRACT

The main goal of this research is to provide a more detailed investigation of the size-dependent response of magneto-electro-thermo-elastic (METE) nanobeams subjected to propagating wave, employing sinusoidal shear deformation beam theory (SSDBT). With the aim to consider the size influences of the structure, the nonlocal strain gradient theory (NSGT) is utilized. Hamilton's principle within constitutive relations of METE materials is incorporated to derive the governing equations. Utilizing Maxwell's relation and magnet-electric boundary conditions, proper distributions for magnetic and electric potentials along the nanobeam are obtained. Thereafter an exact analysis is used to obtain the axial and flexural dispersion relations of METE nanobeams. In numerical results, detailed investigations of wave dispersion behavior related to three modes are addressed. In addition, a relation is introduced to determine the cut-off frequency of the system. Moreover, the effectiveness of various parameters including length scale and nonlocal parameters, nanobeam thickness, and the loadings due to imposed thermo-electro-magnetic field on the response of propagating wave in METE nanobeams are examined.

1. Introduction

Smart materials such as piezoelectric, shape memory and magnetostrictive alloys are the most promising materials which have drawn serious attention in a broad range of engineering

* Corresponding author:
E-mail address: rtalebi@iust.ac.ir (R. Talebitooti)

http://dx.doi.org/10.22064/tava.2020.104267.1128

technologies especially in sensors, and actuators, vibration control and nanotechnology. The reason behind this matter is that, compared to the other conventional materials, rare and phenomenal nature namely adaptive and self-sensing capabilities could be detected for smart materials. It should be noted that smart materials possess an intrinsic coupling effect and interfaces with different fields. Consequently, these materials are adaptive, because of their ability to change the energy types from one to another. [1-5].

Among common smart materials, magneto-electro-elastic (MEE) materials are of interest because of their three-phase coupling effect between magnetic, electric, and mechanical fields [6]. Besides, as the magneto-electric coupling effect is not found in single-phase piezoelectric and piezomagnetic materials, recently MEE materials have made much interest of study among researchers. It is worth mentioning that MEE nanostructures represent different mechanical, electrical, magnetic, physical and chemical properties in comparison with their bulk [7-10].

Due to its high values of wave frequencies about the terahertz order, wave propagation in nano-dimensional problems is extensively being attracted among the researchers. Besides, engineers are able to discover failings or defects in structures via separating waves thanks to the fabulous properties of the response of nano-structures subjected to propagating waves [11]. Moreover, the wave distribution curves of the nano-structures make it possible to explore directly many physical and dynamical properties of them including optical transition and electrical conductance. Hence, it is of great importance to explore the exact characteristics of nano-structures regarding the wave propagation approach [12-14].

It has been previously shown [15] that the predicted results according to NSGT in nano-devices, have satisfying compliance with the results deduced by simulations of molecular dynamics (MD). It should be mentioned that recently some studies have been conducted to consider the effect of the thickness (i.e. strain gradient along z-direction) in the formulation of nano-structures to acquire exact response [15-17].

Accordingly, many previous works related to wave propagation in nano-scale structures have been taken place throughout the world during recent years. For example, Ebrahimi and Barati [18] presented wave dispersion in FG nanobeam applied to longitudinal magnetic field according to Euler-Bernoulli assumptions together with the nonlocality approach. They studied the effects of elastic foundation, material composition, nonlocal feature and external longitudinal magnetic loading on the wave propagation characteristics. Zhang et al. [19] examined the response of piezoelectric nanoplate applied to longitudinal propagating wave regarding nonlocality in conjunction with surface elasticity. Wave propagation analysis of a carbon nanotube (CNT) was presented by Wang [20]. Both Euler-Bernoulli and Timoshenko nonlocal models were developed in the analysis. Li et al. [21] examined the response of viscoelastic CNT in the presence of propagating wave and magnetic field using NSGT. It should be noted that the surface influences are taken into account in their research. Also, utilizing the Euler-Bernoulli assumptions and NSGT, the examination of flexural wave dispersion in FG nanobeam was performed by Li et al. [22]. Wave propagation in inhomogeneous FG nanoplate was examined by Ebrahimi et al. [23] in the framework of NSGT and four-variable refined plate theory. They considered that the nanoplate is in the presence of thermal force in nonlinear form and explored the role of temperature distribution in the wave propagation response. Xiao et al. [24] studied the influence of the NSGT on the propagation features of the viscoelastic monolayer graphene sheet interacted with in-plane waves. Employing higher-order beam theory of Reddy incorporated with NSGT,

She et al. studied the wave dispersion response of FG porous beams in Nanoscale. The role of various involved parameters including volume fraction of porosity and power law index were investigated in the analysis [25]. Karami et al. conducted a research to analyze the wave propagation phenomenon in FG nanoplates using the for-variable refined plate theory and NSGT. The influences of factors such as imposed magnetic potential and gradient index on the dispersion curves were discussed in their investigation [26]. Additionally, some more studies involving the wave performance of structures with Nano dimensions could be found in the available literature [27-36].

Furthermore, the mechanical behavior of nano-structures associated with MEE materials has evoked considerable interest and attention in many studies, recently. Among these works, buckling and vibration problems have been sufficiently studied. However, there exist few studies focusing on the response of such structures in propagating wave existence. For instance, Ebrahimi et al. [37] examined the flexural wave propagation of FG-MEE nanobeams employing NET in conjunction with Euler-Bernoulli beam theory. Furthermore, hiring NET, Arefi [38] explored the effects of applying magneto-electric filed on wave propagation characteristics of FG-MEE nano-rod. Ma et al. [7] have recently explored the wave propagation in MEE nanobeams. Two beam models (i.e. Timoshenko and Euler-Bernoulli) in nonlocal form have been taken into account in this work. Moreover, Ebrahimi and Dabbagh [11] presented wave propagation analysis in the flexural mode for smart FG-MEE nanoplates. They utilized NSGT and shear deformation theory of plate in higher-order form in their investigation. In this work, a parameter study has been investigated for various factors including size-dependency parameters of nonlocal and length scale and magneto-electric potential. Moreover, the effects of these parameters on dispersion characteristics of nanoplates were illustrated in detail. Arefi and Zenkour [40] analyzed the problem of wave dispersion in FG-MEE nanobeam resting on Visco-Pasternak substrate exploiting Timoshenko model as well as the surface elasticity theory.

The conducted literature review discloses that, although some research on wave dispersion properties of nano-scale MEE structures could be found in the literature, there exists not any detailed examination dealing with the wave dispersion response of METE nanobeams subjected to temperature change based on SSDBT and NSGT. Consequently, this research is devoted to fill the mentioned blank in the open literature on wave dispersion of smart nano-scale beams specifically those made of METE material. The size-dependency phenomenon of nanobeam is captured using NSGT. Employing Hamilton's principle incorporating with constitutive relations of METE materials, the governing equations are acquired. Afterwards, the obtained equations are analytically solved to extract the axial and flexural dispersion relations of the nanobeam. As a result, a mathematical relation is presented to calculate the cut-off frequency. Finally, some findings are reported to emphasize the effects of different parameters, for instance, nonlocal and length scale parameters, external magneto-electric loadings and temperature change on longitudinal, shear and bending wave characteristics of METE nanobeam. As a paramount result, it is found that the external magneto-electric potential could considerably affect the dispersion characteristics of the nanobeam. Moreover, compared to the external magneto-electric potential, temperature change has no sensible effect on the properties of dispersing wave.

2. Modeling of the problem

As mentioned before, NSGT shows good compliance with the molecular dynamics (MD) prediction for the size-dependency of nano-scaled structures behavior. Totally, Ke et al. [39] presented the size-dependent constitutive relations for MEE materials in integral form. However, utilizing a proper kernel function, an equivalent differential form of the constitutive relations is widely used for modeling such materials [37]. Therefore, for the sake of convenience, simplified constitutive relations of METE solids in the framework of NSGT can be written as [7]:

$$(1-(e_0a)^2\nabla^2)\sigma_{ij} = (1-l^2\nabla^2)(c_{ijkl}\varepsilon_{kl} - e_{mij}E_m - q_{nij}H_n - \beta_{ij}\Delta T), \tag{1}$$

$$(1-(e_0a)^2\nabla^2)D_i = (1-l^2\nabla^2)(e_{ikl}\varepsilon_{kl} + s_{im}E_m + d_{in}H_n + p_i\Delta T), \tag{2}$$

$$(1-(e_0a)^2\nabla^2)B_i = (1-l^2\nabla^2)(q_{ikl}\varepsilon_{kl} + d_{im}E_m + \mu_{in}H_n + \lambda_i\Delta T). \tag{3}$$

where $\sigma_{ij}, \varepsilon_{ij}, D_i, E_i, B_i$ and H_i correspond to the stress, strain, electric displacement, electric field, magnetic induction and magnetic field, respectively. In addition $c_{ijkl}, e_{mij}, s_{im}, q_{ij}, d_{ij}, \mu_{ij}, p_i, \lambda_i$ and β_{ij} represent elastic, piezoelectric, dielectric, piezo-magnetic, magneto-electric, magnetic, pyro-electric, pyro-magnetic, thermal moduli, respectively and ΔT denotes temperature change. In above equations, e_0a and l respectively indicates nonlocal factor and length scale factor.

Regarding Eqs. (1) to (3), nonlocal strain gradient stress-strain equations of METE nanobeam could be developed as:

$$(1-(e_0a)^2\frac{\partial^2}{\partial x^2})\sigma_{xx} = (1-l^2\frac{\partial^2}{\partial x^2})(\bar{c}_{11}\varepsilon_{xx} - \bar{e}_{31}E_z - \bar{q}_{31}H_z - \bar{\beta}_1\Delta T), \tag{4}$$

$$(1-(e_0a)^2\frac{\partial^2}{\partial x^2})\sigma_{xz} = (1-l^2\frac{\partial^2}{\partial x^2})(\bar{c}_{44}\gamma_{xz} - \bar{e}_{15}E_x - \bar{q}_{15}H_x), \tag{5}$$

$$(1-(e_0a)^2\frac{\partial^2}{\partial x^2})D_z = (1-l^2\frac{\partial^2}{\partial x^2})(\bar{e}_{31}\varepsilon_{xx} + \bar{s}_{33}E_z + \bar{d}_{33}H_z + \bar{p}_3\Delta T), \tag{6}$$

$$(1-(e_0a)^2\frac{\partial^2}{\partial x^2})B_z = (1-l^2\frac{\partial^2}{\partial x^2})(\bar{q}_{31}\varepsilon_{xx} + \bar{d}_{33}E_z + \bar{\mu}_{33}H_z + \bar{\lambda}_3\Delta T). \tag{7}$$

where the reduced coefficients are defined as following [7]:

$$\begin{aligned}
&\bar{c}_{11} = c_{11} - \frac{c_{13}^2}{c_{33}}, \bar{e}_{31} = e_{31} - \frac{c_{13}e_{33}}{c_{33}}, \ \bar{q}_{31} = q_{31} - \frac{c_{13}q_{33}}{c_{33}}, \ \bar{\beta}_1 = \beta_1 - \frac{c_{13}\beta_3}{c_{33}}, \ \bar{c}_{44} = c_{44}, \\
&\bar{e}_{15} = e_{15}, \ \bar{q}_{15} = q_{15}, \ \bar{s}_{33} = s_{33} - \frac{e_{33}^2}{c_{33}}, \ \bar{d}_{33} = d_{33} + \frac{q_{33}e_{33}}{c_{33}}, \ \bar{p}_3 = p_3 + \frac{\beta_3 e_{33}}{c_{33}}, \\
&\bar{\mu}_{33} = \mu_{33} + \frac{q_{33}^2}{c_{33}}, \ \bar{\lambda}_3 = \lambda_3 + \frac{\beta_3 q_{33}}{c_{33}}
\end{aligned} \tag{8}$$

In Fig. (1), METE nanobeam of thickness h is schematically shown. The considered beam is applied to propagating wave, magneto-electric field and temperature change:

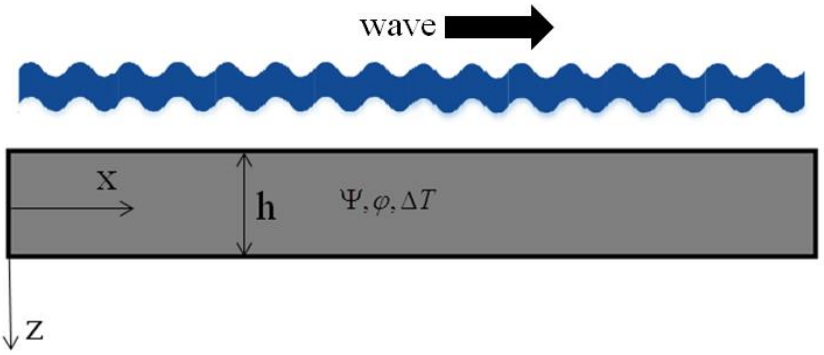

Fig. 1 Geometry of METE nanobeam under propagating wave.

Based on SSDBT, the axial displacement u_x and the transverse displacement u_z are defined as:

$$u_x(x,z,t) = u(x,t) - z\frac{\partial w(x,t)}{\partial x} + R(z)\Phi(x,t), \\ u_z(x,z,t) = w(x,t) \tag{9}$$

where u and w denote axial and transverse displacements of any point on the neutral axis; Φ is the transverse shear strain of any point on the neutral axis; R is a function of z characterizing the transverse shear and distribution of stress along the thickness of the nanobeam; and t is the time.

It should be noted that in Eq. (1), $R(z)$ and Φ are defined as:

$$R(z) = \frac{h}{\pi}\mathrm{Sin}(\frac{\pi z}{h}),\ \ \Phi(x,t) = \frac{\partial w(x,t)}{\partial x} - \varphi(x,t) \tag{10}$$

Equation (1) gives the following strain-displacement relations:

$$\varepsilon_{xx} = \frac{\partial u}{\partial x} - z\frac{\partial^2 w}{\partial x^2} + R(z)\frac{\partial \Phi}{\partial x}, \\ \gamma_{xz} = \frac{dR(z)}{dz}\Phi(x,t) \tag{11}$$

It is supposed that the nanobeam is polarized only in z direction; therefore the in-plane magnetic and electric field is ignored, i.e., $E_x = H_x = 0$. Hence, the variation of strain energy is expressed as [7]:

$$\delta U_s = \int_0^L \int_{-h/2}^{h/2} (\sigma_{xx}\delta\varepsilon_{xx} + \sigma_{xz}\delta\gamma_{xz} - D_z\delta E_z - B_z\delta H_z)dzdx \tag{12}$$

where on the basis of Maxwell's equation, E_z and H_z are given by:

$$E_z = -\frac{\partial \Psi}{\partial z},\ H_z = -\frac{\partial \varphi}{\partial z} \tag{13}$$

It is valuable to note that Ψ and φ are electric and magnetic potentials, respectively. As it is seen by the means of Maxwell's equation, the relationships between electric / magnetic potential and electric / magnetic field are established.

Substituting Eqs. (3) and (5) into Eq. (4), we have:

$$\begin{aligned}\delta U_s = &\int_0^L \int_{-h/2}^{h/2} \sigma_{xx}\delta\left(\frac{\partial u}{\partial x} - z\frac{\partial^2 w}{\partial x^2} + R(z)\frac{\partial \Phi}{\partial z}\right)dzdx + \\ &\int_0^L \int_{-h/2}^{h/2} \sigma_{xz}\left(\frac{dR}{dz}\right)\delta\Phi dzdx + \int_0^L \int_{-h/2}^{h/2} D_z\delta\frac{\partial \Psi}{\partial z}dzdx + \int_0^L \int_{-h/2}^{h/2} B_z\delta\frac{\partial \phi}{\partial z}dzdx\end{aligned} \tag{14}$$

The first variation of the virtual kinetic energy of the considered nanobeam can be written as:

$$\begin{aligned}\delta T_b = &\int_0^L \left\{ m_0\left(\frac{\partial u}{\partial t}\delta\frac{\partial u}{\partial t} + \frac{\partial w}{\partial t}\delta\frac{\partial w}{\partial t}\right) + m_2\frac{\partial^2 w}{\partial x\partial t}\delta\frac{\partial^2 w}{\partial x\partial t}\right. \\ &\left. -\frac{24m_2}{\pi^3}\left(\frac{\partial^2 w}{\partial x\partial t}\delta\frac{\partial \Phi}{\partial t} + \frac{\delta\partial^2 w}{\partial x\partial t}\frac{\partial \Phi}{\partial t}\right) + \frac{6m_2}{\pi^2}\frac{\partial \Phi}{\partial t}\delta\frac{\partial \Phi}{\partial t}\right\}dx\end{aligned} \tag{15}$$

where m_0 and m_2 are the mass inertias defined as:

$$m_0 = \int_{-h/2}^{h/2} \rho dz,\ m_2 = \int_{-h/2}^{h/2} \rho z^2 dz \tag{16}$$

In addition, the variation of the external work related to the imposed magneto-electric potential and temperature change is written by the following equation:

$$\delta\Pi_f = \int_0^L \left\{ (N_e + N_m + N_T)\frac{\partial w}{\partial x}\frac{\partial \delta w}{\partial x} \right\} \tag{17}$$

Where

$$N_e = \bar{e}_{31}V_0, N_m = \bar{q}_{31}\Omega_0, N_T = -\bar{\beta}_1 h\Delta T. \tag{18}$$

In accordance with Hamiltonian's principle, the following relation is written:

$$\int_0^t \delta(U_s - T_b + \Pi_f) = 0 \tag{19}$$

By substituting Eqs. (14), (15) and (17) to Eq. (19), based on integration by parts and setting the coefficients of $\delta u, \delta w, \delta\Phi, \delta\Psi$ and $\delta\varphi$ equal to zero, equations of motion are obtained as:

$$-\frac{\partial N_{xx}}{\partial x} + m_0\frac{\partial^2 u}{\partial t^2} = 0, \tag{20}$$

$$\begin{aligned}&\frac{\partial^2 M_{xx}^b}{\partial x^2} + (N_e + N_m + N_T)\frac{\partial^2 w}{\partial x^2} = \\ &m_0\frac{\partial^2 w}{\partial t^2} - m_2\frac{\partial^4 w}{\partial x^2\partial t^2} + \frac{24m_2}{\pi^3}\frac{\partial^3 \Phi}{\partial t^2\partial x}\end{aligned} \tag{21}$$

$$\frac{\partial M_{xx}^s}{\partial x} - Q = \frac{6m_2}{\pi^2}\frac{\partial^2 \Phi}{\partial t^2} - \frac{24m_2}{\pi^3}\frac{\partial^3 w}{\partial x\partial t^2} \tag{22}$$

$$\frac{\partial D_z}{\partial z} = 0 \tag{23}$$

$$\frac{\partial B_z}{\partial z} = 0 \tag{24}$$

In which variables N_{xx}, Q, M^b_{xx} and M^s_{xx} are expressed by:

$$N_{xx} = \int_{-h/2}^{h/2} \sigma_{xx} dz,\ M^b_{xx} = \int_{-h/2}^{h/2} \sigma_{xx} z dz,\ M^s_{xx} = \int_{-h/2}^{h/2} \sigma_{xx} R(z) dz,\ Q = \int_{-h/2}^{h/2} \sigma_{xz} \frac{dR(z)}{dz} dz \tag{25}$$

Considering Eqs. (6) and (7), Eqs. (23) and (24) are solved to achieve magnetic and electric potential distribution as:

$$\frac{\partial^2 \Psi}{\partial z^2} = M_1 (-\frac{\partial^2 w}{\partial x^2} + \frac{\partial \Phi}{\partial x}\frac{dR}{dz}) \tag{26}$$

$$\frac{\partial^2 \phi}{\partial z^2} = M_2 (-\frac{\partial^2 w}{\partial x^2} + \frac{\partial \Phi}{\partial x}\frac{dR}{dz}) \tag{27}$$

in which

$$\begin{aligned} M_1 &= (\bar{e}_{31}\bar{\mu}_{33} - \bar{d}_{33}\bar{q}_{31}) / (\bar{s}_{33}\bar{\mu}_{33} - \bar{d}^2_{33}) \\ M_2 &= (\bar{s}_{33}\bar{q}_{31} - \bar{d}_{33}\bar{e}_{31}) / (\bar{s}_{33}\bar{\mu}_{33} - \bar{d}^2_{33}) \end{aligned} \tag{28}$$

Boundary conditions corresponding to the applied magnetic and electric potentials are chosen to be as:

$$\begin{aligned} &\Psi(h/2) = V_0,\ \Psi(-h/2) = 0 \\ &\varphi(h/2) = \Omega_0,\ \varphi(-h/2) = 0 \end{aligned} \tag{29}$$

Thus, by applying Eq. (29) to Eqs. (26) and (27), magnetic and electric potential distributions along the thickness of the nanobeam are obtained as:

$$\Psi = -\frac{M_1}{2}\frac{\partial^2 w}{\partial x^2}(z^2 - \frac{h^2}{4}) - M_1 \frac{\partial \Phi}{\partial x}\frac{h^2}{\pi^2}\cos(\frac{\pi z}{h}) + \frac{V_0}{h} z + \frac{V_0}{2} \tag{30}$$

$$\Psi = -\frac{M_1}{2}\frac{\partial^2 w}{\partial x^2}(z^2 - \frac{h^2}{4}) - M_1 \frac{\partial \Phi}{\partial x}\frac{h^2}{\pi^2}\cos(\frac{\pi z}{h}) + \frac{V_0}{h} z + \frac{V_0}{2} \tag{31}$$

Incorporating Eqs. (25), (4) and (5) results in the following relationship:

$$(1-(e_0 a)^2 \frac{\partial^2}{\partial x^2}) N_{xx} = (1 - l^2 \frac{\partial^2}{\partial x^2}) \left\{ \bar{c}_{11} h \frac{\partial u}{\partial x} + \bar{e}_{31} V_0 + \bar{q}_{31} \Omega_0 - \beta_1 h \Delta T \right\} \tag{32}$$

$$(1-(e_0 a)^2 \frac{\partial^2}{\partial x^2}) M^b_{xx} = (1 - l^2 \frac{\partial^2}{\partial x^2}) \left\{ -\tilde{c}_{11} \frac{h^3}{12} \frac{\partial^2 w}{\partial x^2} + \tilde{c}_{11} \frac{2h^3}{\pi^3} \frac{\partial \Phi}{\partial x} \right\} \tag{33}$$

$$(1-(e_0 a)^2 \frac{\partial^2}{\partial x^2}) M^s_{xx} = (1 - l^2 \frac{\partial^2}{\partial x^2}) \left\{ -\tilde{c}_{11} \frac{2h^3}{\pi^3} \frac{\partial^2 w}{\partial x^2} + \tilde{c}_{11} \frac{h^3}{2\pi^3} \frac{\partial \Phi}{\partial x} \right\} \tag{34}$$

$$(1-(e_0 a)^2 \frac{\partial^2}{\partial x^2}) Q = (1 - l^2 \frac{\partial^2}{\partial x^2}) \frac{h}{2} \bar{c}_{44} \Phi \tag{35}$$

in which

$$\tilde{c}_{11} = \bar{c}_{11} + \bar{e}_{31} M_1 + \bar{q}_{31} M_2 \tag{36}$$

By substituting Eq. (32) into Eq. (20), consequently inserting Eqs. (33) and (34) into Eqs. (21) and (22), the equations of motion for METE nanobeam based on SSDBT and NSGT are extracted as:

$$\bar{c}_{11} h (1 - l^2 \frac{\partial^2}{\partial x^2}) \frac{\partial^2 u}{\partial x^2} = (1 - (e_0 a)^2 \frac{\partial^2}{\partial x^2}) m_0 \frac{\partial^2 u}{\partial t^2} \tag{37}$$

$$\begin{aligned} &(1 - l^2 \frac{\partial^2}{\partial x^2}) \left\{ -\tilde{c}_{11} \frac{h^3}{12} \frac{\partial^4 w}{\partial x^4} + \tilde{c}_{11} \frac{2h^3}{\pi^3} \frac{\partial^3 \Phi}{\partial x^3} \right\} + \\ &(1 - (e_0 a)^2 \frac{\partial^2}{\partial x^2}) \left\{ (N_e + N_m + N_T) \frac{\partial^2 w}{\partial x^2} \right\} = \\ &(1 - (e_0 a)^2 \frac{\partial^2}{\partial x^2}) \left\{ m_0 \frac{\partial^2 w}{\partial t^2} - m_2 \frac{\partial^4 w}{\partial x^2 \partial t^2} + \frac{24 m_2}{\pi^3} \frac{\partial^3 \Phi}{\partial t^2 \partial x} \right\} \end{aligned} \tag{38}$$

$$\begin{aligned} &(1 - l^2 \frac{\partial^2}{\partial x^2}) \left\{ -\tilde{c}_{11} \frac{2h^3}{\pi^3} \frac{\partial^3 w}{\partial x^3} + \tilde{c}_{11} \frac{h^3}{2\pi^3} \frac{\partial^2 \Phi}{\partial x^2} \right\} - \\ &(1 - l^2 \frac{\partial^2}{\partial x^2}) \left\{ \frac{h}{2} \bar{c}_{44} \Phi \right\} = (1 - (e_0 a)^2 \frac{\partial^2}{\partial x^2}) \left\{ \frac{6 m_2}{\pi^2} \frac{\partial^2 \Phi}{\partial t^2} - \frac{24 m_2}{\pi^3} \frac{\partial^3 w}{\partial x \partial t^2} \right\} \end{aligned} \tag{39}$$

As it is seen governing motion equations of the nanobeam are derived completely. In the next section, the wave propagation problem for the considered nanobeam is solved and then the wave dispersion relationships are obtained.

3. Analytical solution and dispersion relations

In order to investigate the properties of dispersing wave, the solution of the equations of motion is considered to be in the following form:

$$\begin{Bmatrix} u(x,t) \\ w(x,t) \\ \Phi(x,t) \end{Bmatrix} = \begin{Bmatrix} \bar{U} e^{i(kx - \omega t)} \\ \bar{W} e^{i(kx - \omega t)} \\ \bar{\Phi} e^{i(kx - \omega t)} \end{Bmatrix} \tag{40}$$

As it was shown in the previous section, Eq. (37) is decoupled from the other two governing equations. Hence substituting $u(x,t)$ in Eq. (37) leads to one of the axial wave frequency (longitudinal wave frequency):

$$\omega^2 = \frac{\bar{c}_{11} h k^2 + \bar{c}_{11} h k^4 l^2}{m_0 + m_0 (e_0 a)^2 k^2} \tag{41}$$

Inserting $w(x,t)$ and $\Phi(x,t)$ into Eqs. (38) and (39) deduces the other wave dispersion relation as:

$$\begin{bmatrix} H_{11} & H_{12} \\ H_{21} & H_{22} \end{bmatrix} \begin{Bmatrix} \bar{\Phi} \\ \bar{W} \end{Bmatrix} \times e^{i(kx-\omega t)} = 0 \tag{42}$$

Where

$$\begin{aligned} H_{11} &= \tilde{c}_{11}\frac{h^3}{2\pi^3}k^2 + \frac{h}{2}\bar{c}_{44} + l^2\tilde{c}_{11}\frac{h^3}{2\pi^3}k^4 + \frac{h}{2}l^2\bar{c}_{44}k^2 - \frac{6m_2}{\pi^2}\omega^2 - (e_0a)^2\frac{6m_2}{\pi^2}\omega^2k^2 \\ H_{21} &= H_{12} = -\tilde{c}_{11}\frac{2h^3}{\pi^3}ik^3 - l^2\tilde{c}_{11}\frac{2h^3}{\pi^3}ik^5 + \frac{24m_2}{\pi^3}ik\omega^2 + e_0a^2\frac{24m_2}{\pi^3}i\omega^2k^3 \\ H_{22} &= -\tilde{c}_{11}\frac{h^3}{12}k^4 - l^2\tilde{c}_{11}\frac{h^3}{12}k^6 - (N_e + N_m + N_T)k^2 \\ &-(e_0a)^2(N_e + N_m + N_T)k^4 + m_0\omega^2 + \\ &m_2\omega^2k^2 + (e_0a)^2m_0\omega^2k^2 + (e_0a)^2m_2\omega^2k^4 \end{aligned} \tag{43}$$

Therefore by setting the determinant of the matrix in the left-hand side of Eq. (42) to be zero, one can calculate the flexural wave frequencies (shear and bending wave frequencies) of the nanobeam:

$$\begin{vmatrix} H_{11} & H_{12} \\ H_{21} & H_{22} \end{vmatrix} = 0 \tag{44}$$

Second flexural wave frequency starts a nonzero value called cut-off frequency. Cut-off frequency can be calculated by the use of the following relation:

$$\omega_{cut-off} = \sqrt{\frac{\pi^2}{12}\frac{h\bar{c}_{44}}{m_2}} \tag{45}$$

As it is clear, the applied magneto-electric potential and temperature change exhibit no influence on the value of cut-off frequency. This property is only dependent on material and geometrical properties of the nanobeam ($\bar{c}_{44}, h$).

4. Numerical results and discussion

This section is dedicated to discuss the numerical results for the wave propagating in METE nanobeams using SSDBT and NSGT. The considered nanobeam is constructed of two-phase $BiTiO_3$-$CoFe_2O_4$ for which the material properties are tabulated in Table 1 [7]. The thickness of the nanobeam is assumed to be 10 nm. The effects of the nonlocal parameter e_0a, length-scale parameter l, electric potential V_0, magnetic intensity Ω_0 and temperature variation ΔT on the dispersion characteristics (wave frequency, phase velocity, cut-off wave number) of the nanobeam are discussed in detail in following subsections. Firstly, in order to examine the precision and reliability of the solution method, phase velocity diagram for a carbon nanotube (CNT) is presented in Fig. (2), where the results of the current solution are compared with those discussed in Ref. [23]. The geometrical and properties of the CNT is chosen based on the reference. The validation study reveals that the obtained results agree well with those presented in the reference and as a consequence, the utilized numerical solution is accurate enough to predict reliable response.

4.1. First wave frequency (longitudinal wave frequency)

Considering various values of the nonlocal parameter $e_0 a$, the dispersion relation between the wave number and axial wave frequency is investigated and the results are shown in Fig. (3) for $l = 0nm$ and $l = 2nm$. As expected, the decreasing influence of the nonlocal factor on the wave frequency is evident. It is worth pointing out that this effect is more significant at higher wave number values ($k \geq 0.2nm^{-1}$). In comparison with the nonlocal parameter $e_0 a$, length scale parameter l acts in a vice versa way. To put it differently, considering this parameter makes the frequency increase. With attention to Eq. (38), one can understand that by tending wave number to infinity (when the length scale parameter l sets to be zero and $e_0 a \neq 0$), the wave frequency gives a constant value. This behavior mentioned above, can be clearly observed in Fig. (4). This frequency is called escape frequency. The variation of escape frequency versus the nonlocal parameter is plotted in Fig. (5). It can be concluded from the figure that, if the nonlocal parameter changes from 0 to 1 nm, the slope of the diagram is higher than once the nonlocal parameter changes from 1 to 2. It means that the decrease in escape frequency is more significant at lower values of nonlocal factor. It should be mentioned that decreasing / increasing effect of the nonlocal factor / length scale factor comes from the stiffness softening / stiffness hardening effect covered by NSGT.

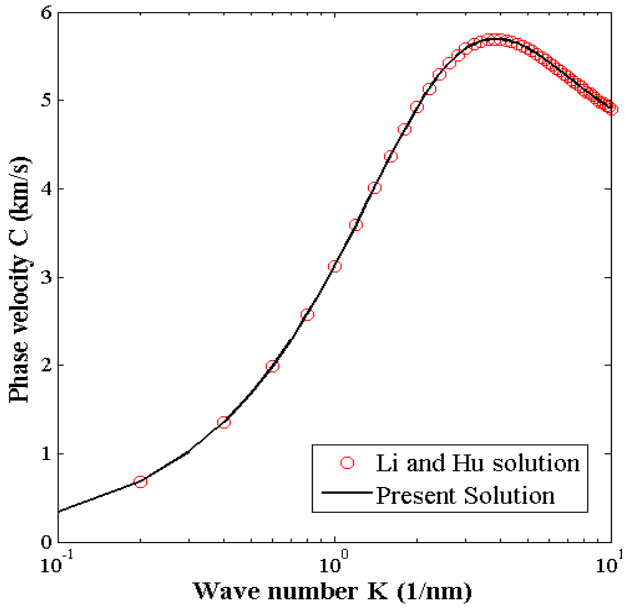

Fig 2. Verification study for phase velocity of SWCNT armchair (5, 5) with Ref. [23], with $ea = 0.4\ nm$, $l = 0.13\ nm$.

Table 1. Material properties of $BiTiO_3$–$CoFe_2O_4$ material

Properties	Values
Elastic constant (Gpa)	c_{11}=132, c_{12}=71,c_{13}=73, c_{22}=132, c_{33}=115, c_{44}=c_{55}=25.6, c_{66}=30.5
Piezoelectric constant(C/m^2)	e_{31}= -4.1,e_{32}=-4.1,e_{33}=14.1, e_{15}=e_{24}=10.5
Dielectric constant(10^{-9} C/Vm)	s_{11}=s_{22}=5.841, s_{33}=7.124
Piezomagnetic constant(N/Am)	q_{15}=275, q_{31}=290.1, q_{33}= 349.9
Magneto-electric constant(10^{-12} Ns/VC)	d_{11}=5.367,d_{33}=2737.5
Magnetic constant(10^{-6} Ns^2/C^2)	μ_{11}= -297,μ_{33}=83.5
Thermal moduli constant(10^5 N/Km^2)	β_1=4.738, β_2=4.738, β_3=4.529
Pyroelectric constant(10^{-6} C/N)	P_3=25
Pyromaagnetic constant(10^{-6}N/AmK)	λ_3=5.19
Mass density(10^3 kg/m^3)	ρ=5.55

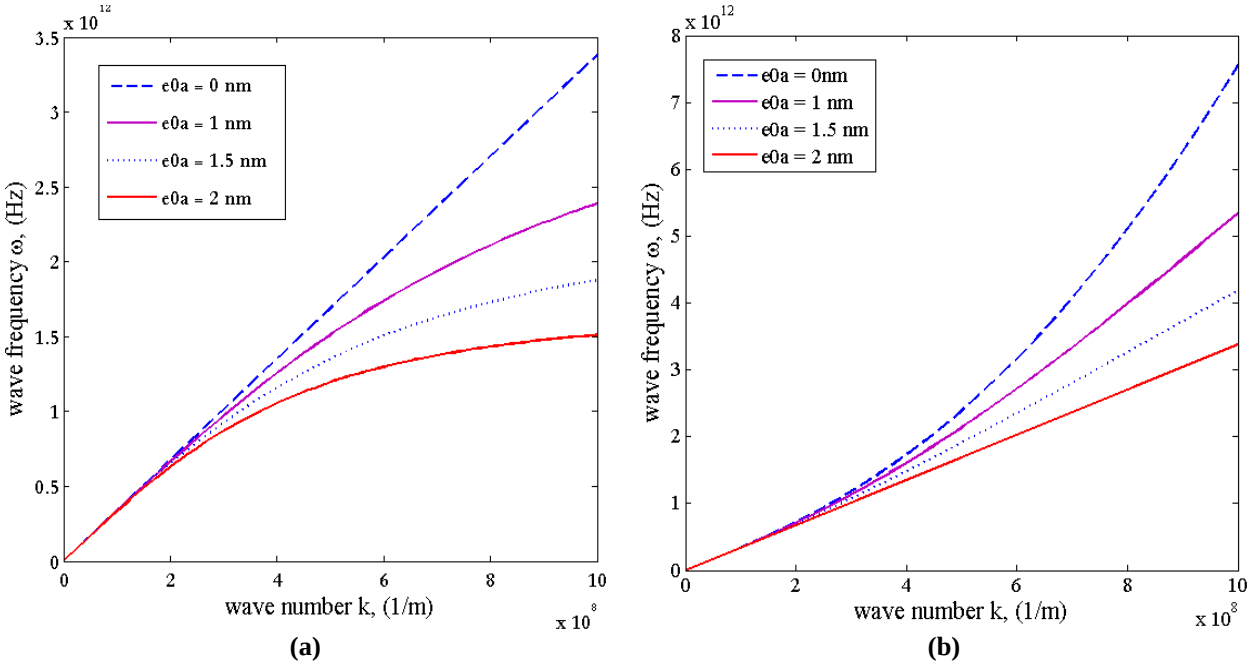

Fig 3. Variation of axial wave frequency of nanobeam with h = 10 nm versus wave number for different nonlocal factors: **(a)** $l = 0nm$ and **(b)** $l = 2nm$.

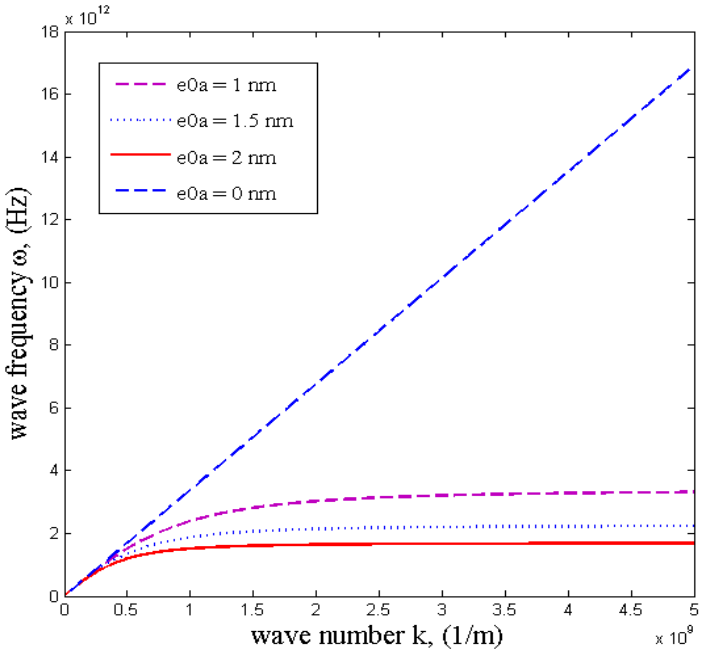

Fig 4. Variation of axial wave frequency versus wave number for different nonlocal parameters with h = 10 nm and l = 0 nm.

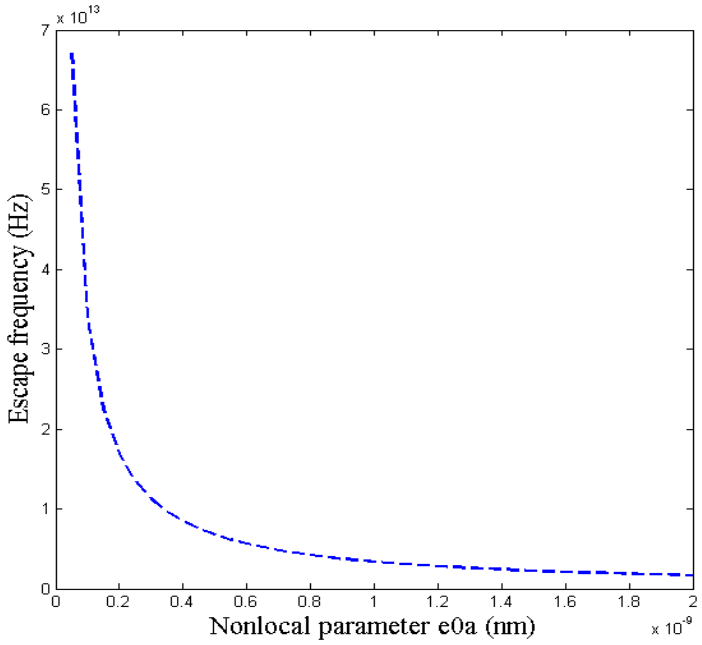

Fig 5. Variation of escape frequency of the nanobeam versus nonlocal parameter when h = 10 nm and l =0.

4.2. Shear and bending wave frequencies

In this subsection, the dispersion characteristics of first and second flexural modes (shear and bending modes) are investigated. For this aim, dispersion relations of two flexural modes (wave frequency and phase velocity diagrams) for different nonlocal parameters and length scale parameters are plotted. Figure 6 examines the nonlocal parameter effect on the first flexural wave frequency variation versus the wave number. In addition, variations of the first flexural phase velocity as a function of wave number are demonstrated in Fig. (7), considering various nonlocal and length scale parameters. As it is shown, the nonlocal parameter / length scale parameter exerts stiffness-softening / stiffness-hardening effect and therefore leads to lower / higher wave frequencies or phase velocities. It should be noted that this behavior was observed in the previous subsection in analyzing dispersion relations of axial wave frequency. The other obtained result is that for higher values of wave numbers (almost $k \geq 0.18 nm^{-1}$) the first phase velocity is damped.

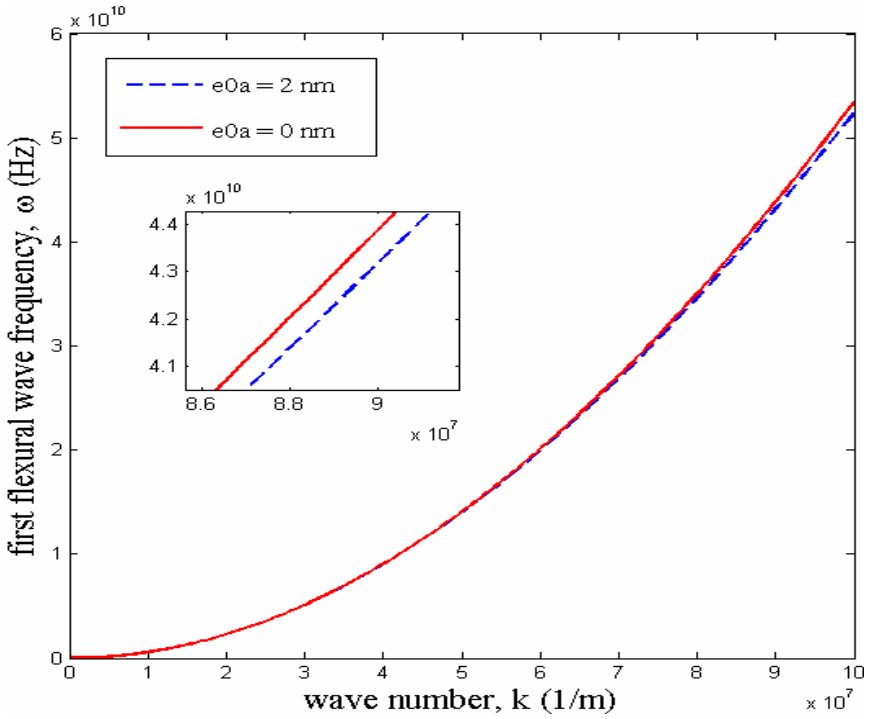

Fig 6. Variation of first flexural wave frequency of nanobeam versus wave number with and without nonlocal parameter when h = 5 nm and l=2.

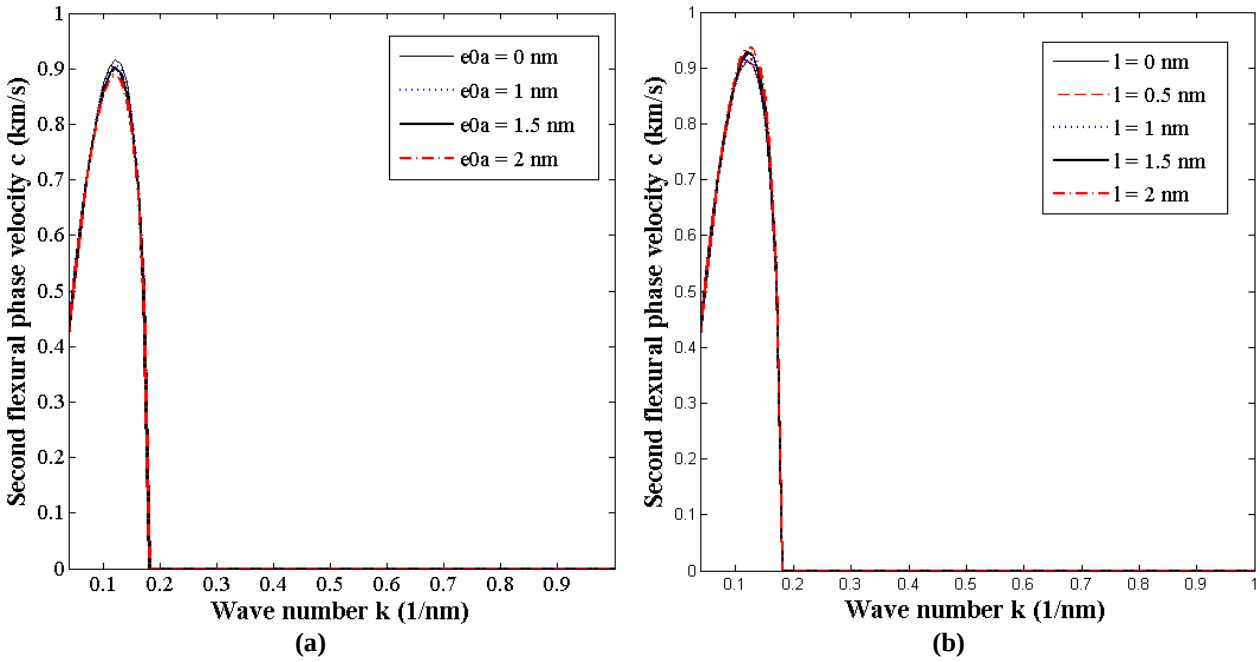

Fig 7. Variation of first flexural phase velocity of nanobeam with h = 10 nm versus wave number: (a) for different nonlocal factors with $l = 0.5nm$ and (b) for different length scale parameters with $e_0 a = 0.5nm$.

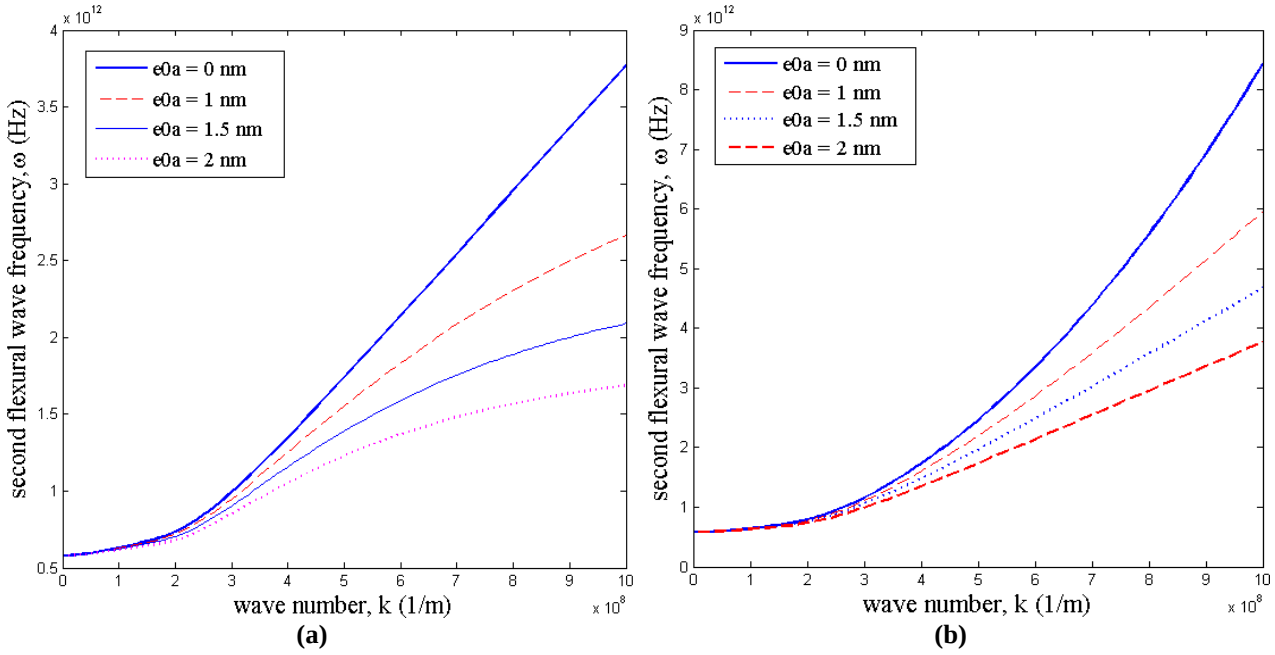

Fig 8. Variation of second flexural wave frequency of nanobeam with h = 10 nm versus wave number for different nonlocal parameters: **(a)** with $l = 0nm$ and **(b)** with $l = 2nm$.

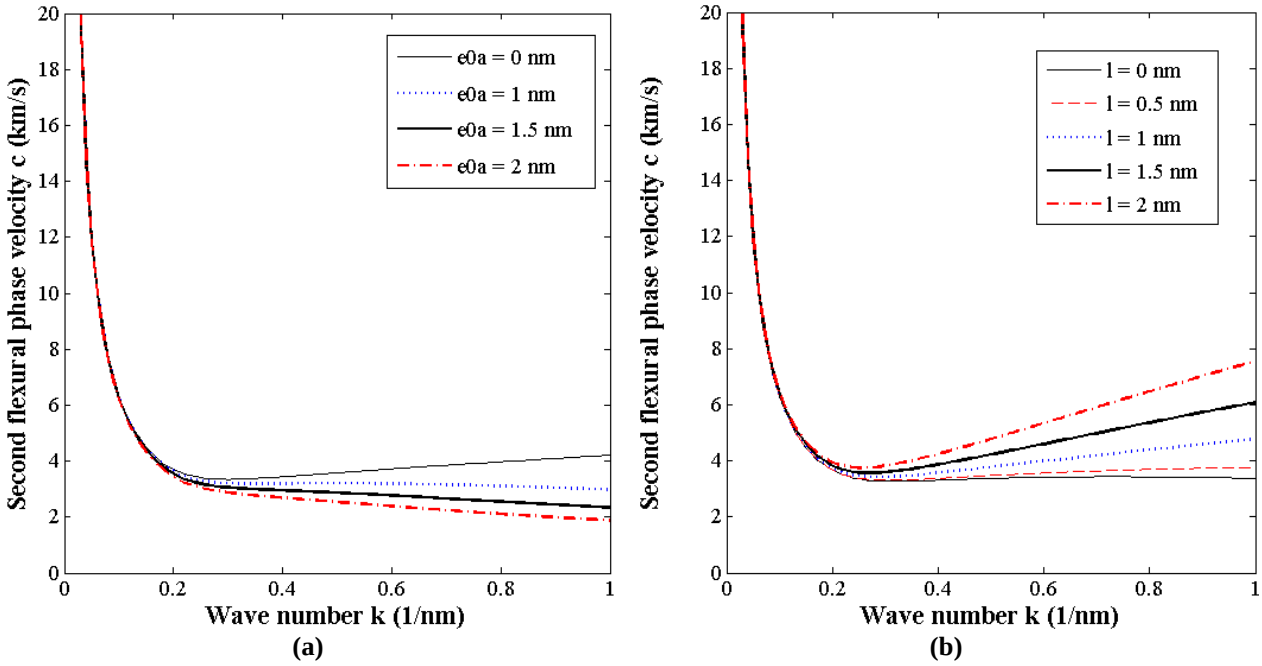

Fig 9. Variation of second flexural phase velocity of nanobeam with h = 10 nm with respect to wave number: (a) for various nonlocal factors with $l = 0.5nm$ and (b) for various length scale factors with $e_0 a = 0.5nm$.

Figures (8) and (9) illustrate the variations of second flexural wave frequency and phase velocity respectively. As it is seen, various values for length scale and nonlocal factors are considered for the analysis. It is observed that for lower amounts of the wave number ($k \le 0.2\,\mathrm{nm}^{-1}$), the obtained wave frequency and phase velocity for distinct amounts of nonlocal or length scale parameters are identical. Furthermore, the difference between phase velocities (or wave numbers) for various values of length scale and the nonlocal parameter is obvious when the amount of wave numbers exceeds $0.2nm^{-1}$. The other prominent result is that in higher wave numbers, the size-dependent parameters have more effects on the phase velocity of the nanobeam. In other words, the difference between classical and size-dependent values of phase velocity (or wave frequency) is more significant in higher wave numbers. According to the diagrams plotted in Fig. (8), it is found out that the second flexural wave frequency starts a nonzero value called cut-off frequency. Besides, obtained relation for cut-off frequency (see Eq. (42)) implies that the only effective parameters on cut-off frequency are $m_2, \bar{c}_{44}$ and the nanobeam thickness h. It means that the other parameters including nonlocal parameter, length scale parameter, external magnetic and electric potentials and temperature change play no role in changing the cut-off frequency's value. On the other hand, $\bar{c}_{44}$ is constant for the material. Thus, it is concluded that the only parameter affecting the cut-off wave frequency is nanobeam thickness. Therefore diagram of cut-off wave frequency as a function of nanobeam thickness is plotted in Fig. 10. As depicted in the figure, the cut-off frequency decreases when the thickness is increased. Besides, the decreasing rate of the wave frequency is considerable at low values of thicknesses.

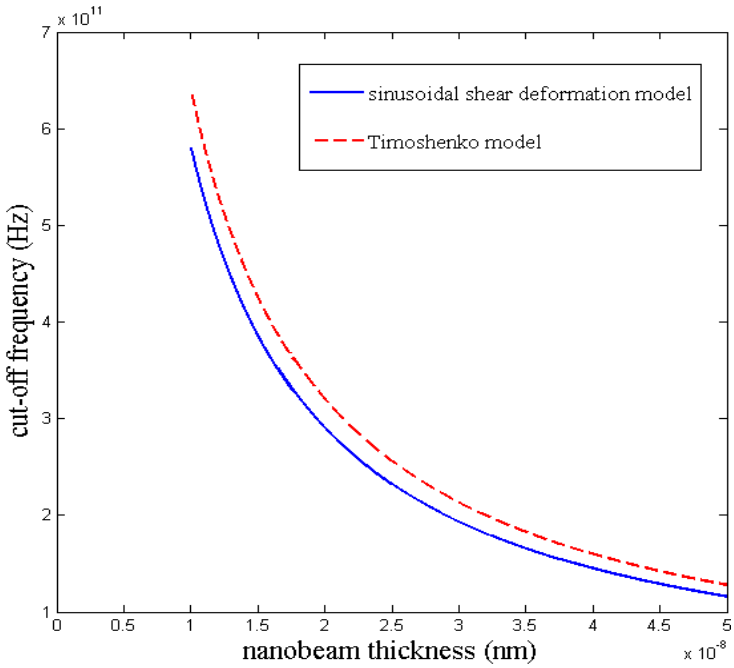

Fig 10. Variation of cut-off frequency versus nanobeam's thickness.

4.3. magneto-electric and temperature change effects on the wave dispersion relation

METE smart materials are sensitive to external magnetic and electric potentials and also temperature change. Consequently, it is worthwhile to study the influences of these parameters on the characteristics of propagating waves in the considered structure. Therefore, in this subsection, it is focused on exploring the effects of the imposed electric / magnetic potential and temperature change on the dispersion relation between phase velocity / wave frequency and wave number.

Dispersion relations between first flexural wave frequency and wave number are presented in Figs. (11) and (12) respectively for various values of electric and magnetic potentials. The nonlocal and length scale parameters are set to be 1 nm in the analysis. It can be obviously seen that the increase of the applied electric / magnetic potential leads to decrease / increase in the nanobeams' wave frequency. This comes from the compressive and tensile forces affecting the overall stiffness of the nanobeam. The other result found from the figures is that, when positive / negative amounts of electric / magnetic potential is applied, the imaginary part of the first flexural wave frequency becomes nonzero. Moreover, it is revealed that, for positive / negative values of electric / magnetic potential, the cut-off wave number's position shifts to right. In other words, the wave number attributed to the cut-off phenomenon becomes nonzero. It is concluded that, increasing the positive / negative electric / magnetic potential makes the cut-off frequency increase. The reason might be the compressive axial force which is generated in the nanobeam by applying positive electric / negative magnetic potential. This force exerts a softening effect in the system. Figure (13) illustrates the variations of the first flexural phase velocity versus the wave number for various amounts of electric and magnetic potential. The effect of the applied potentials is clear especially for lower amounts of the wave number. Figure (14) is allotted to explore the effect of temperature change on the wave relation between first flexural wave

frequency and wave number in the absence of an electro-magnetic field. It is easily concluded that, unlike the applied potentials, the temperature change shows no sensible influence on the wave frequency.

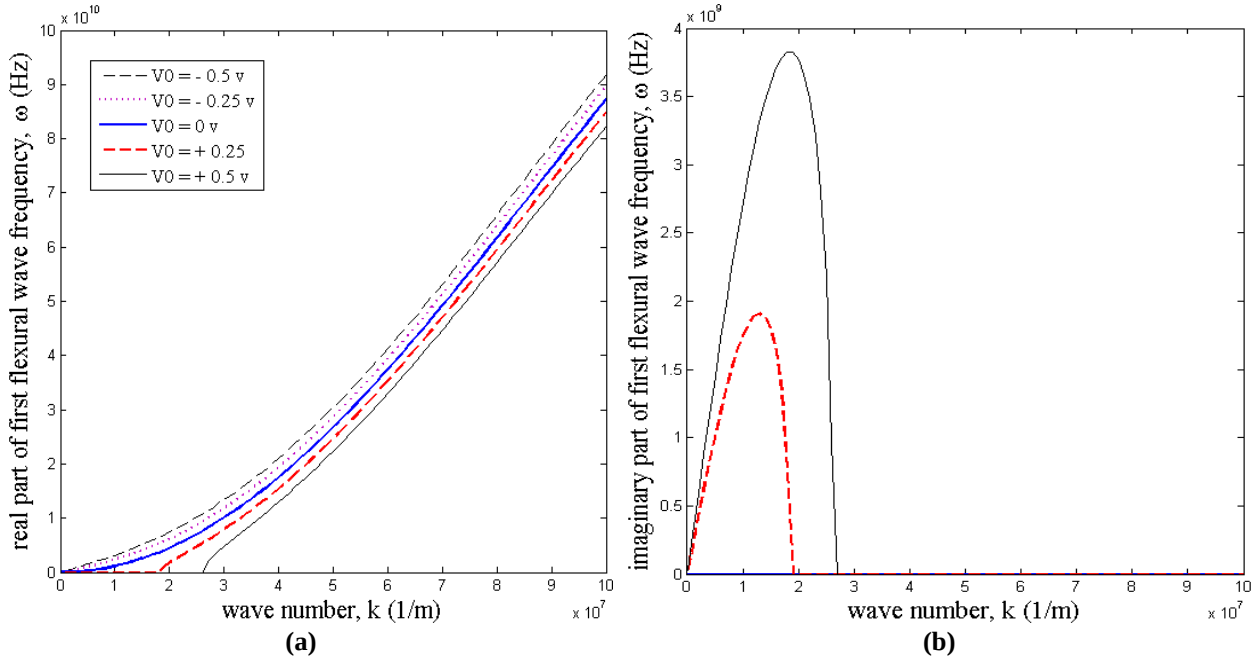

Fig 11. Dispersion relation between first flexural wave frequency and wave number considering various amounts of electric potential V_0 with $\Omega_0 = 0$, h= 10 nm, $e_0 a$ = 1 nm and l = 1 nm: **(a)** real part and **(b)** imaginary part.

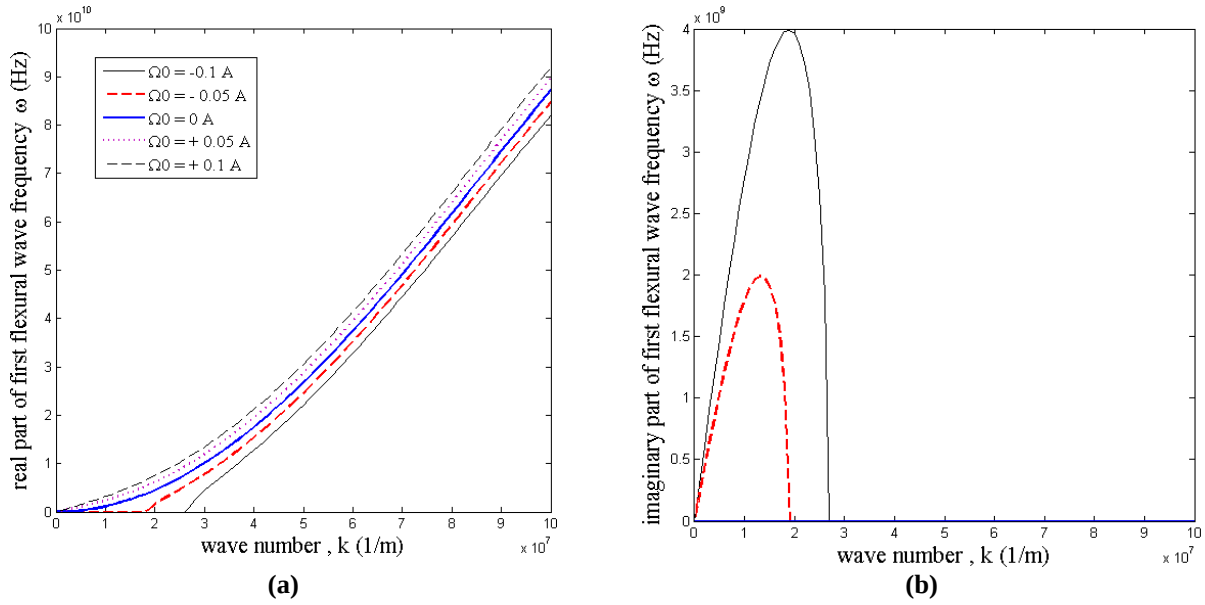

Fig 12. Dispersion relation between first flexural wave frequency and wave number considering various amounts of magnetic potential Ω_0 with $V_0 = 0$, h= 10 nm, $e_0 a$ = 1 nm and l = 1 nm: **(a)** real part and **(b)** imaginary part.

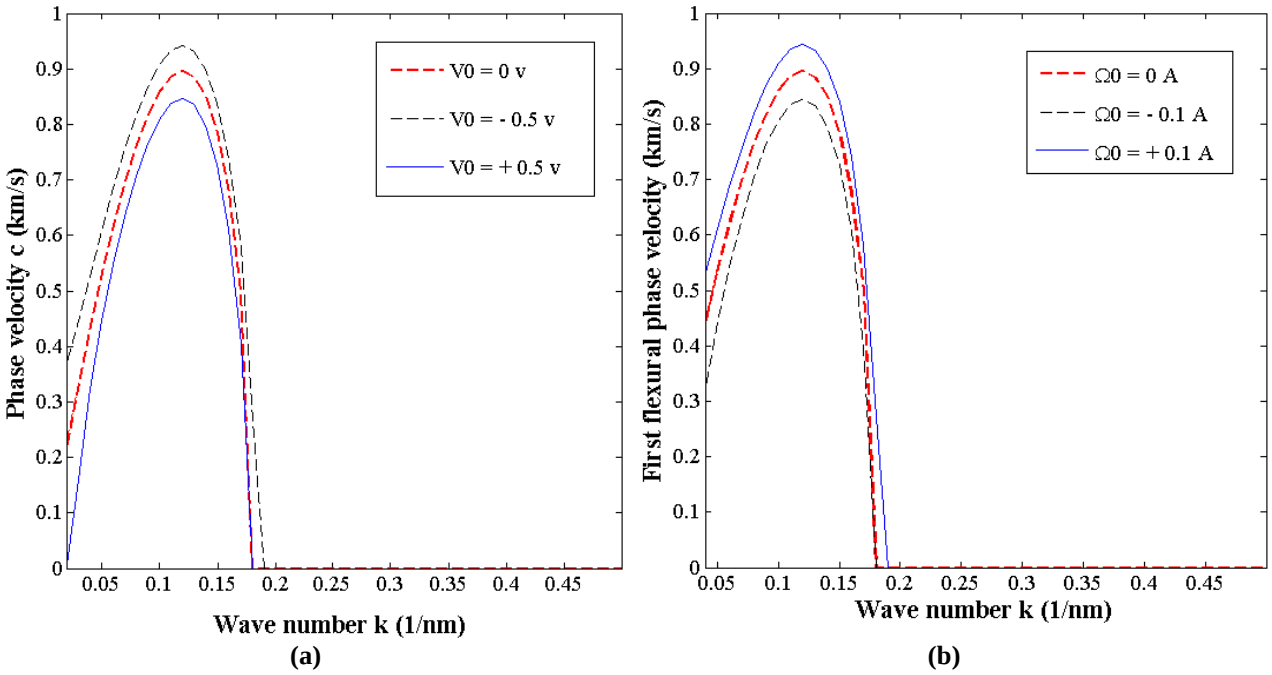

Fig 13. Dispersion relation between wave number and first flexural phase velocity considering h= 10 nm, $e_0 a$ = 1 nm and l = 1 nm: (a) for different amounts of electric potential (b) for different values of magnetic potential.

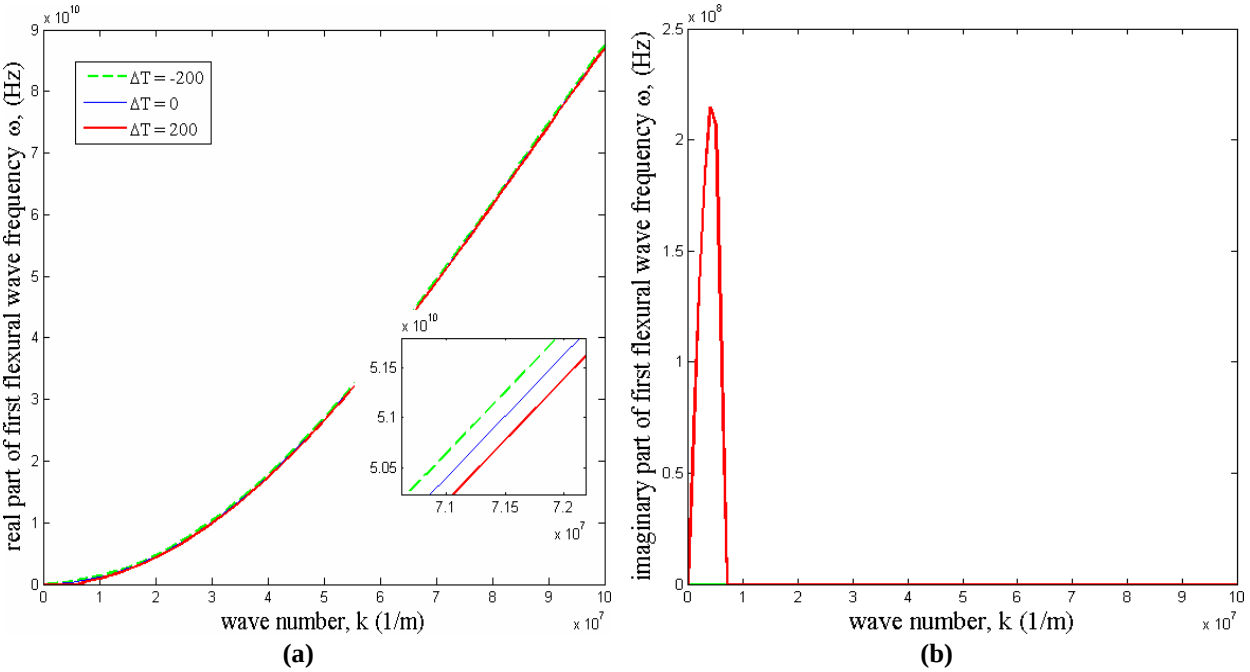

Fig 14. Dispersion relation between first flexural wave number and wave frequency for different temperature changes ΔT with $V_0 = \Omega_0 = 0$, h= 10 nm, $e_0 a$ = 1 nm and l = 1 nm: (a) real part and (b) imaginary part.

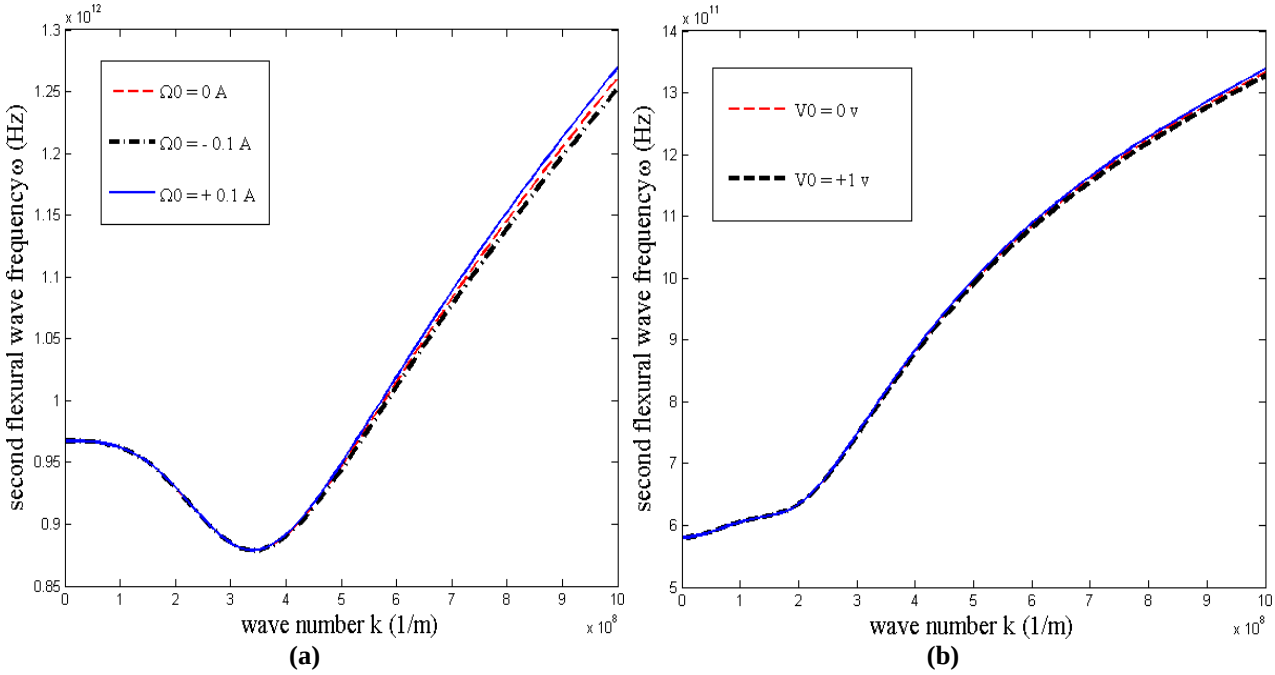

Fig 15. Dispersion relation between wave number and second flexural wave frequency with e_0a = 3 nm and l = 0.5 nm: **(a)** for different amounts of magnetic potential with h = 6 nm **(b)** for different amounts of electric potential with h = 10 nm.

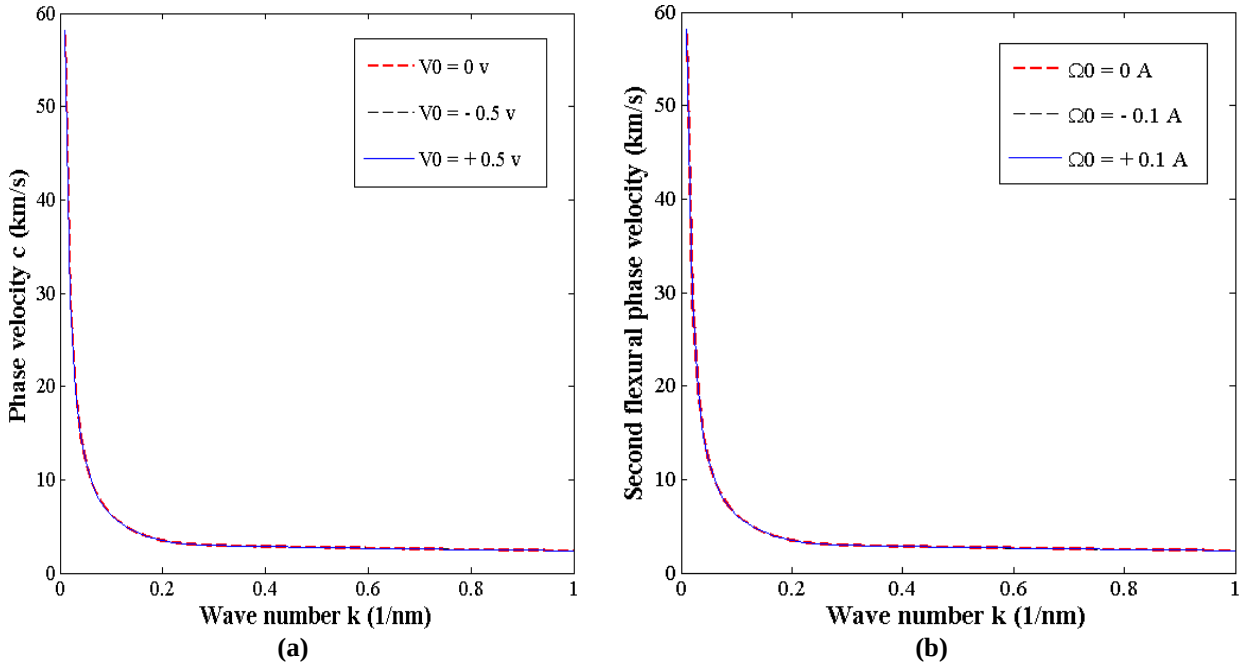

Fig 16. Dispersion relation between wave number and second flexural phase velocity with e_0a = 3 nm and l = 0.5 nm: **(a)** for different amounts of electric potential with h = 6 nm **(b)** for different amounts of electric potential with h = 10 nm.

Figures (15) and (16) indicate dispersion relations (wave frequency-wave number or phase velocity-wave number) of the second flexural mode considering various values of magnetic and electric potential for nanobeam thicknesses of 6 and 10 nm. By comparing the diagrams shown in Figs (15a) and (15b) it is deduced that, the effectiveness of imposed potentials on the second dispersion relation is more considerable for nanobeam with lower thickness. Moreover, this impact is sensible for the domain of wave numbers with higher amounts. However, in comparison with the first mode, it can be seen that the effect of the applied potentials on the second mode dispersion relation is less.

Finally, the influences of nonlocal factor $e_0 a$, length scale factor l and magneto-electric field on the cut-off phenomenon are discussed. For this purpose, the variations of first flexural frequency versus the wave number for the nanobeam with $h = 5nm$ and $h = 10nm$ considering various values of $e_0 a$ and l are illustrated in Fig. (17). As it is seen, considering nonlocal factor / length scale factor makes cut-off wave number decrease / increase. For the case of nanobeam with greater thickness, $e_0 a$ and l have no considerable impact on cut-off wave number. Herewith, diagrams of the cut-off wave number as a function of magnetic field / electric field are depicted in Figs. (18) and (19). These figures present decreasing / enhancing impact of magnetic field / electric field on cut-off wave number. This could be ascribed to stiffness-hardening / stiffness-softening influence of imposed positive magnetic / negative electric field. The reason is the axial tensile / compressive force generated by positive magnetic / negative electric potential which affects the stiffness of the system.

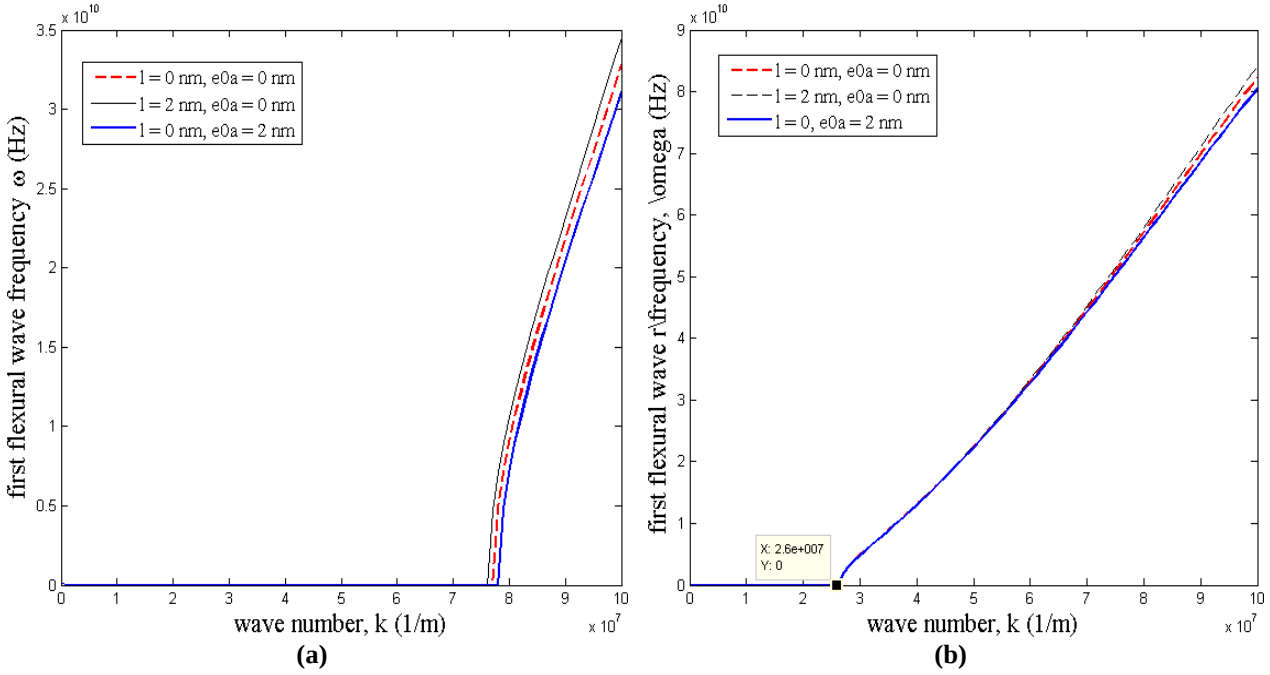

Fig 17. Influence of size-dependent factors on cut-off wave number with $V_0 = \Omega_0 = 0$ **(a)** h= 5 nm **(b)** h = 10 nm.

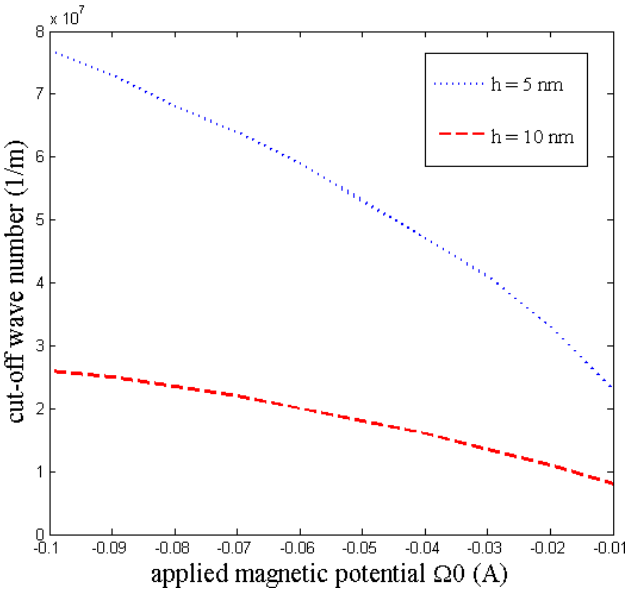

Fig 18. Cut-off wave number variation versus magnetic field Ω_0 with e_0a = 2 nm, l = 1 nm.

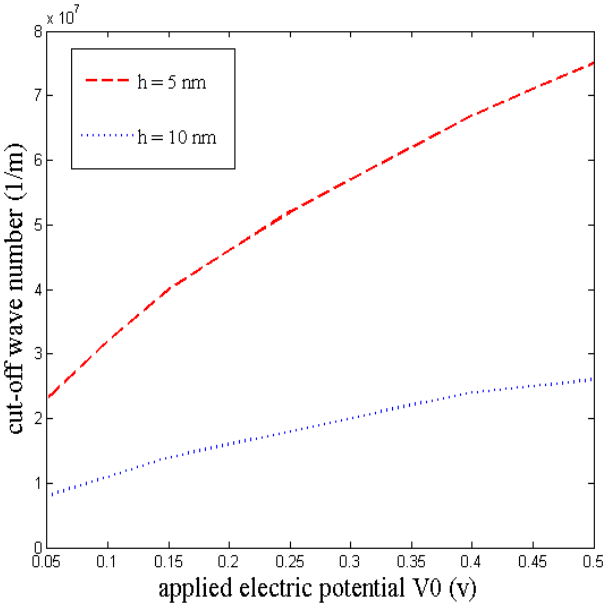

Fig 19. Cut-off wave number variation versus electric filed with = 1.5 nm, = 1 nm.

5. Conclusion

In this study, the wave propagation characteristics of METE nanobeams were investigated according to size-dependency. For deriving equations of motion of the system, SSDBT was established in conjunction with NSGT combined with Hamilton's principle and constitutive relations of METE materials. Thereafter, the governing motion equations were analytically solved to obtain the axial and flexural dispersion relations (wave frequency vs. wave number or phase velocity vs. wave number). Besides, a mathematical relation was introduced to determine the cut-off frequency. A numerical investigation is devoted to explore the influences of nonlocal and length scale factors, electro-magnetic field, and temperature change on the wave dispersion response were also investigated. The numerical results indicated that by increasing the nonlocal factor / length scale factor, the wave frequency, as well as phase velocity, tends to decrease / increase. It was revealed that in a particular flexural mode the effects of size-dependent parameters (nonlocal and length scale) are more visible for a domain of wave numbers with higher amounts. Also, among the flexural modes, the nonlocal and length scale influences are more pronounced for higher modes. Moreover, size-dependent parameters could have a significant influence on cut-off wave number only for the nanobeams with smaller thicknesses. Totally, applying positive / negative electric field led to reduction / increment in the wave frequency and also phase velocity values. However, the magnetic potential acts in the opposite way. The utilization of positive electric / magnetic potential led to a softer / stiffer nanobeam. This phenomenon made the cut-off wave number nonzero by applying positive electric / negative magnetic potential. Furthermore, by decreasing / increasing the value of negative magnetic / positive electric field, the cut-off wave number decreased / increased. Unlike the applied potentials, temperature change had no considerable influence on wave dispersion relation.

Finally, as a prominent result it was found that the effects of applied potentials on flexural wave dispersion relation were more considerable for lower modes. Totally, the analysis may be helpful for increasing a deep knowledge about the accurate wave dispersion response of smart METE nanobeams. This may lead to an accurate and efficient design of the structures benefiting from such smart nano-scaled beams.The authors declare that they have no conflict of interest.

References

[1] J. Chen, P. Heyliger, E. Pan, Free vibration of three-dimensional multilayered magneto-electro-elastic plates under combined clamped/free boundary conditions, Journal of Sound and Vibration, 333 (2014) 4017-4029.
[2] M. Fakhari, N. Saeedi, A. Amiri, Size-dependent vibration and instability of magneto-electro-elastic nano-scale pipes containing an internal flow with slip boundary condition, International Journal of Engineering, 29 (2016) 995-1004.
[3] A. Daga, N. Ganesan, K. Shankar, Behaviour of magneto-electro-elastic sensors under transient mechanical loading, Sensors and Actuators A: Physical, 150 (2009) 46-55.
[4] M.-F. Liu, An exact deformation analysis for the magneto-electro-elastic fiber-reinforced thin plate, Applied Mathematical Modelling, 35 (2011) 2443-2461.
[5] A. Amiri, I. Pournaki, E. Jafarzadeh, R. Shabani, G. Rezazadeh, Vibration and instability of fluid-conveyed smart micro-tubes based on magneto-electro-elasticity beam model, Microfluidics and Nanofluidics, 20 (2016) 38.
[6] A. Jandaghian, O. Rahmani, Free vibration analysis of magneto-electro-thermo-elastic nanobeams resting on a Pasternak foundation, Smart Materials and Structures, 25 (2016) 035023.
[7] L.-H. Ma, L.-L. Ke, Y.-Z. Wang, Y.-S. Wang, Wave propagation in magneto-electro-elastic nanobeams via two nonlocal beam models, Physica E: Low-dimensional Systems and Nanostructures, 86 (2017) 253-261.
[8] A. Amiri, R. Shabani, G. Rezazadeh, Coupled vibrations of a magneto-electro-elastic micro-diaphragm in micro-pumps, Microfluidics and Nanofluidics, 20 (2016) 18.
[9] A. Milazzo, An equivalent single-layer model for magnetoelectroelastic multilayered plate dynamics, Composite Structures, 94 (2012) 2078-2086.
[10] M. Arefi, A.H. Soltan Arani, Higher order shear deformation bending results of a magnetoelectrothermoelastic functionally graded nanobeam in thermal, mechanical, electrical, and magnetic environments, Mechanics Based Design of Structures and Machines, 46 (2018) 669-692.
[11] F. Ebrahimi, A. Dabbagh, On flexural wave propagation responses of smart FG magneto-electro-elastic nanoplates via nonlocal strain gradient theory, Composite Structures, 162 (2017) 281-293.
[12] N. Sina, H. Moosavi, H. Aghaei, M. Afrand, S. Wongwises, Wave dispersion of carbon nanotubes conveying fluid supported on linear viscoelastic two-parameter foundation including thermal and small-scale effects, Physica E: Low-dimensional Systems and Nanostructures, 85 (2017) 109-116.
[13] J. Chen, J. Guo, E. Pan, Wave propagation in magneto-electro-elastic multilayered plates with nonlocal effect, Journal of Sound and Vibration, 400 (2017) 550-563.
[14] H. Liu, Z. Lv, Q. Li, Flexural wave propagation in fluid-conveying carbon nanotubes with system uncertainties, Microfluidics and Nanofluidics, 21 (2017) 140.
[15] L. Li, H. Tang, Y. Hu, The effect of thickness on the mechanics of nanobeams, International Journal of Engineering Science, 123 (2018) 81-91.
[16] H. Tang, L. Li, Y. Hu, Coupling effect of thickness and shear deformation on size-dependent bending of micro/nano-scale porous beams, Applied Mathematical Modelling, 66 (2019) 527-547.
[17] H. Tang, L. Li, Y. Hu, W. Meng, K. Duan, Vibration of nonlocal strain gradient beams incorporating Poisson's ratio and thickness effects, Thin-Walled Structures, 137 (2019) 377-391.
[18] F. Ebrahimi, M.R. Barati, Magnetic field effects on nonlocal wave dispersion characteristics of size-dependent nanobeams, Applied Physics A, 123 (2017) 81.

[19] J. Zang, B. Fang, Y.-W. Zhang, T.-Z. Yang, D.-H. Li, Longitudinal wave propagation in a piezoelectric nanoplate considering surface effects and nonlocal elasticity theory, Physica E: Low-dimensional Systems and Nanostructures, 63 (2014) 147-150.
[20] Q. Wang, Wave propagation in carbon nanotubes via nonlocal continuum mechanics, Journal of Applied Physics, 98 (2005) 124301.
[21] L. Li, Y. Hu, L. Ling, Wave propagation in viscoelastic single-walled carbon nanotubes with surface effect under magnetic field based on nonlocal strain gradient theory, Physica E: Low-dimensional Systems and Nanostructures, 75 (2016) 118-124.
[22] L. Li, Y. Hu, L. Ling, Flexural wave propagation in small-scaled functionally graded beams via a nonlocal strain gradient theory, Composite Structures, 133 (2015) 1079-1092.
[23] F. Ebrahimi, M.R. Barati, A. Dabbagh, A nonlocal strain gradient theory for wave propagation analysis in temperature-dependent inhomogeneous nanoplates, International Journal of Engineering Science, 107 (2016) 169-182.
[24] W. Xiao, L. Li, M. Wang, Propagation of in-plane wave in viscoelastic monolayer graphene via nonlocal strain gradient theory, Applied Physics A, 123 (2017) 388.
[25] G.-L. She, K.-M. Yan, Y.-L. Zhang, H.-B. Liu, Y.-R. Ren, Wave propagation of functionally graded porous nanobeams based on non-local strain gradient theory, The European Physical Journal Plus, 133 (2018) 368.
[26] B. Karami, D. Shahsavari, M. Janghorban, Wave propagation analysis in functionally graded (FG) nanoplates under in-plane magnetic field based on nonlocal strain gradient theory and four variable refined plate theory, Mechanics of Advanced Materials and Structures, 25 (2018) 1047-1057.
[27] A. Ghorbanpour Arani, M. Jamali, M. Mosayyebi, R. Kolahchi, Analytical modeling of wave propagation in viscoelastic functionally graded carbon nanotubes reinforced piezoelectric microplate under electro-magnetic field, Proceedings of the Institution of Mechanical Engineers, Part N: Journal of Nanomaterials, Nanoengineering and Nanosystems, 231 (2017) 17-33.
[28] H. Zeighampour, Y.T. Beni, I. Karimipour, Wave propagation in double-walled carbon nanotube conveying fluid considering slip boundary condition and shell model based on nonlocal strain gradient theory, Microfluidics and Nanofluidics, 21 (2017) 85.
[29] L. Li, Y. Hu, Wave propagation in fluid-conveying viscoelastic carbon nanotubes based on nonlocal strain gradient theory, Computational Materials Science, 112 (2016) 282-288.
[30] F. Kaviani, H.R. Mirdamadi, Wave propagation analysis of carbon nano-tube conveying fluid including slip boundary condition and strain/inertial gradient theory, Computers & Structures, 116 (2013) 75-87.
[31] Y.-X. Zhen, Wave propagation in fluid-conveying viscoelastic single-walled carbon nanotubes with surface and nonlocal effects, Physica E: Low-dimensional Systems and Nanostructures, 86 (2017) 275-279.
[32] L. Wang, Wave propagation of fluid-conveying single-walled carbon nanotubes via gradient elasticity theory, Computational Materials Science, 49 (2010) 761-766.
[33] A.G. Arani, M. Roudbari, S. Amir, Longitudinal magnetic field effect on wave propagation of fluid-conveyed SWCNT using Knudsen number and surface considerations, Applied Mathematical Modelling, 40 (2016) 2025-2038.
[34] F. Ebrahimi, M.R. Barati, Wave propagation analysis of quasi-3D FG nanobeams in thermal environment based on nonlocal strain gradient theory, Applied Physics A, 122 (2016) 843.
[35] A. Amiri, R. Talebitooti, L. Li, Wave propagation in viscous-fluid-conveying piezoelectric nanotubes considering surface stress effects and Knudsen number based on nonlocal strain gradient theory, The European Physical Journal Plus, 133 (2018) 252.
[36] A. Masoumi, A. Amiri, R. Talebitooti, Flexoelectric effects on wave propagation responses of piezoelectric nanobeams via nonlocal strain gradient higher order beam model, Materials Research Express, 6 (2019) 1050d1055.

[37] F. Ebrahimi, M.R. Barati, A. Dabbagh, Wave dispersion characteristics of axially loaded magneto-electro-elastic nanobeams, Applied Physics A, 122 (2016) 949.
[38] M. Arefi, Analysis of wave in a functionally graded magneto-electro-elastic nano-rod using nonlocal elasticity model subjected to electric and magnetic potentials, Acta Mechanica, 227 (2016) 2529-2542.
[39] L.-L. Ke, Y.-S. Wang, Free vibration of size-dependent magneto-electro-elastic nanobeams based on the nonlocal theory, Physica E: Low-Dimensional Systems and Nanostructures, 63 (2014) 52-61.